Chemical Engineering Journal 155 (2009) 347–354

Contents lists available at ScienceDirect

Chemical Engineering Journal

journal homepage: www.elsevier.com/locate/cej

Composites as cracking catalysts in the production of biofuel from palm oil: Deactivation studies

Subhash Bhatia*, Abdul Rahman Mohamed, Noor Aisyah Ahmad Shah

School of Chemical Engineering, University Sains Malaysia, Engineering Campus, 14300 Nibong Tebal, S.P.S Penang, Malaysia

ARTICLE INFO

Article history:
Received 2 February 2009
Received in revised form 7 July 2009
Accepted 7 July 2009

Keywords:
Composite catalysts
Catalytic cracking
Deactivation
Biofuel
Activity models

ABSTRACT

Composite catalysts HZSM-5/alumina (CZA) and Al-MCM-41/alumina (CMA) were synthesized and tested for their catalytic cracking activity in the production of biofuel from palm oil. Both composite catalysts were characterized for their structure, acidity and surface morphology. The addition of alumina in the composite catalysts improved their hydrothermal stability due to the changes in the surface morphology. The deactivation of the catalysts was studied by obtaining time on stream data by varying the palm oil to catalyst ratio of 8–16. The deactivation data were analyzed using different activity models and the deactivation parameters were determined.

1. Introduction

The production of biofuel from palm oil has been extensively studied using zeolites as the cracking catalysts [1–8]. Zeolite ZSM-5 has remarkable properties and performance in FCC process [9], and MCM-41 mesoporous material are reported as promising and selective catalysts [2,3] for biofuel production in the catalytic cracking of palm oil due to higher diffusivity of bulky molecules [1–8]. The conventional catalyst for gas oil cracking contains zeolite that provides the major surface area as well as active sites and thus is the key component that controls catalyst activity and selectivity [10]. In order to disperse zeolite in the matrix and to increase its thermal and hydrothermal stabilities, alumina is added as a binder without any chemical bonds between matrix and zeolite. The presence of meso- and macropores in the catalyst is desired to increase the product selectivity during catalytic cracking [11].

ZSM-5/MCM-41 [4] and Beta/MCM-41 [8] as composite catalysts have also been reported in the palm oil cracking because of the growing interest in the ordered porous materials with combined micro- and mesopores due to their significant supplementary advantages. A significant improvement in the selectivity of products was observed. However, one of the major barriers of solid acid catalyst usage in the catalytic cracking reaction is the rapid deactivation of the catalyst. Most of the reactions involving oil fractions, the catalyst deactivates by active site coverage due to coke formation, depending on the catalyst age. The deactivation could be expressed in terms of process time or the deactivating agent i.e., coke on the catalyst, without explicit link to the operating conditions.

The effect of coke could be suppressed by changing the operating parameters of reaction process, for example by increasing pressure and decreasing the cracking conversion/temperature ratio [10]. However, the changes in these process parameters have limitations. Therefore the development of catalyst resistance to coking is an alternative solution to this problem. The understanding of catalyst deactivation allows the development of improved catalysts being less sensitive to the deactivation and perform better.

Since composite catalysts have been investigated for the production of biofuel from palm oil in terms of products selectivity [4,8], therefore it will be interesting to study their catalyst deactivation (stability). The composites composed of low crystalline materials like alumina could help in this respect. In the present study, the catalytic activity, hydrothermal stability and deactivation of the composite catalysts containing HZSM-5, and Al-MCM-41 with alumina as binder in the production of biofuel from palm oil cracking are reported. The effect of time on stream (TOS) on catalyst deactivation is reported and deactivation parameters are obtained using different activity models.

2. Experimental

2.1. Catalyst preparation

2.1.1. Alumina

2 M Al_2O_3 (boehmite sol) was prepared following Yoldas process [12] with some modifications. This method describes a direct preparation of the high-concentration boehmite sol. 21.1 g of aluminum

* Corresponding author. Tel.: +60 4 5996409; fax: +60 4 5941013.
E-mail address: chbhatia@eng.usm.my (S. Bhatia).

1385-8947/$ – see front matter © 2009 Elsevier B.V. All rights reserved.
doi:10.1016/j.cej.2009.07.020

Nomenclature

φ	activity of catalyst
n_d	order of catalyst deactivation constant
k_d	rate of catalyst deactivation constant
Σs^2	sum of error squares

isopropoxide (ALISOP, 98%, Fluka) was slowly added to 50 ml distilled water, which was well stirred and controlled at temperature of 353 K. Large, irregularly shaped clusters started to appear, and gradually precipitated in the flask during the hydrolysis and condensation process when the amount of ALISOP added exceeded 13.2 g. 7 ml of 1 M HNO_3 (that gave the H^+/Al^{3+} ratio of 0.07) was added once the addition of ALISOP was almost completed to disperse the appeared slurry. After that, the ALISOP/water mixture was vigorously stirred for half an hour and heated overnight (12 h) at 363–373 K. This boehmite sol was then modified by adding 1 M HNO_3 with ratio of acid/sol volume is 1:5 and stirred at 348 K for another 1 h.

2.1.2. Al-MCM-41

Mesoporous aluminosilicate material with the Si/Al ratio of 40 was synthesized following the procedure described by Lindlar et al. [13] with modifications. 47.0 g of 1 M sodium hydroxide solution and 5.82 g of Cab-osil M5 were mixed and stirred at 353 K for 2 h. Another mixture was prepared separately by mixing 5.72 g of hexadecyl-trimethyl ammonium bromide (CTABr), 0.19 g of sodium aluminate, 12.0 ml of distilled water and 0.32 g of ammonia solution (25%, Merck) and stirred at 353 K for 1 h. The first mixture was slowly added to the second mixture with vigorous stirring at 370 K. The mixture was stirred for 1 h at 370 K and later heated at 370 K for 24 h without stirring. The mixture was cooled to room temperature and pH was adjusted to about 10.2 by drop wise addition of acetic acid (25%) under vigorous stirring. The reaction mixture was subsequently heated again to 370 K for 24 h. This procedure for pH adjustment and subsequent heating was repeated one more time. The product was filtered, washed and dried at 370 K before being calcined at 823 K for 5 h.

2.1.3. Composites HZSM-5/alumina and Al-MCM-41/alumina

Composite catalysts containing microporous HZSM-5 or mesoporous Al-MCM-41 materials/alumina were prepared following the procedure reported in the literature [14]. HZSM-5 (Zeolyst, Si/Al = 40) or Al-MCM-41 was dispersed in deionized water (20 wt% in aqueous) and the pH was adjusted in the range of 9.5–10 by addition of 1 M NaOH. The samples were stirred for 30 min. The as-prepared HZSM-5 or Al-MCM-41 in water was added drop wise into the alumina gel under stirring, while the pH of the mixture was adjusted in the range of 3.0–3.5 by using HNO_3. The composite is denoted as CYAX with C refers to composite; Y is either Z = HZSM-5 or M = Al-MCM-41; A refers to alumina and X is the alumina weight percentage in the composite synthesis gel. The mixture was then heated to 348 K for 1–1.5 h until the mixture became viscous. The partially gelled mixture was used to prepare the granules by the oil-drop method [14].

The partially gelled mixture was transferred to droppers for the drop formation. The mixture was allowed in the form of drops to descend through a pool of paraffin oil. Spherical wet-gel particles were formed due to the surface tension. The wet-gel particles formed in the oil were passed into the ammonia solution placed right underneath the paraffin oil. After aging in the ammonia solution for at least 1 h, the soft wet-gel particles became rigid. These particles were withdrawn from the ammonia solution, carefully sieved, and washed with water. The washed particles were dried at 318 K for 24 h. The dry particles in the shape of granules were calcined at 823 K for 5 h. The organic compound adhered to the granules was removed during the calcination step. During granulation, the silicalite crystallites were embedded in the alumina network through the oil-drop method. In the present study, the lower ordered mesophase alumina was present in HZSM-5 or Al-MCM-41 as outer layer of spherical composite (granule) and HZSM-5 or Al-MCM-41 as the core, resulted from the granulation process.

In this present study, HZSM-5/alumina with 35 wt% alumina (CZA35) and Al-MCM-41/alumina with 25 wt% (CMA25) compositions are studied due to their best performance in the preliminary palm oil cracking test.

2.2. Characterization and hydrothermal stability

The catalysts were characterized by X-ray diffraction (XRD) to determine the structure and composition of crystalline material using a Philips diffractometer with Cu Kα radiation. The 2θ values of 5–150° were used for HZSM-5 and its composites CZA35, whereas 2θ values of 1–10° for Al-MCM-41 and CMA25 were used with a step of 0.04°/10 s. The acidity of the catalysts was determined using FTIR (PerkinElmer Model 2000) after subjected to pyridine adsorption. A scanning electron microscope (SEM) (Model Leica Cambridge S-360) was employed to examine the surface morphology of samples. Thermal gravimetric analysis (TGA) was used to study the thermal stability of the catalysts (PerkinElmer Thermal Gravimetric Analyzer, TGA 7), the samples were heated from the room temperature to 1173 K at heating rate of 10 K/min. The hydrothermal stability test was conducted by subjecting the catalysts to steam at 1073 K for 1 h prior to activity test in palm oil cracking [7,15].

2.3. Activity test

The cracking activity of the catalysts was measured at reaction temperature of 723 K and weight hourly space velocity, WHSV of 2.5 h^{-1} in a fixed-bed microreactor at atmospheric pressure reported elsewhere [1–8]. HZSM-5/alumina and Al-MCM-41/alumina activities were obtained using palm oil as feed for the activity test. In a typical activity test, 1 g of catalyst was loaded over 0.2 g of quartz wool supported by a stainless steel mesh in the microreactor (185 mm × 10 mm I.D.) placed in the vertical tube furnace (Model No. MTF 10/25/130, Carbolite). Once there was no change in the palm oil conversion at the temperature 723 K, the steady state was reached. There was no deactivation of the catalyst observed during this period. The experiment was repeated to check the reproducibility of the data. The data were reproducible within an experimental error of ±5%. The liquid product was collected in a glass liquid sampler, while the gaseous products were collected in a gas-sampling bulb. The unconverted oil was separated from the liquid product by distillation in a micro-distillation unit (Büchi B850, GKR) at 473 K for 30 min under vacuum (100 Pa) with the pitch as the residual oil. The gaseous products were analyzed over a gas chromatograph (Hewlett Packard, Model 5890 series II) using a HP Plot Q capillary column (Divinyl benzene/styrene porous polymer, 30 m long × 0.53 mm ID × 40 μm film thickness) equipped with a thermal conductivity detector (TCD) and nitrogen as a carrier gas. The organic liquid product (OLP) was analyzed using a capillary glass column (Petrocol DH 50.2, film thickness 0.5 μm, 50 m long × 0.2 mm ID) at a split ratio of 1:100, using a FID detector.

The composition of OLP was defined according to the boiling range of petroleum products in three categories i.e., gasoline fraction (333–393 K), kerosene fraction (393–453 K) and diesel fraction (453–473 K). The boiling range of each fraction was determined by injecting commercial samples of gasoline, kerosene and diesel in gas chromatograph. The spent catalyst was washed with acetone

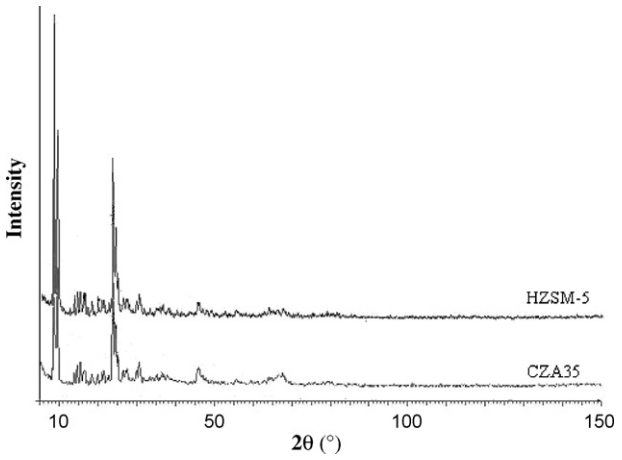

Fig. 1. XRD patterns of HZSM-5 and composite CZA35.

prior to the coke analysis. The amount of coke was determined by the difference in weight before and after calcination in muffle furnace (catalyst regeneration). The spent catalyst was reused by regenerating the catalyst at 823 K for 2 h, in order to remove the coke deposited onto the catalyst.

In order to find out the deactivation behavior of the catalysts, time on stream (TOS) study was carried out over the catalysts. In deactivation experiments, the weight of oil per gram of catalyst was varied from 8 to 16. The catalyst activity was monitored with the time on stream study.

3. Results and discussion

3.1. Catalyst characterization

The XRD diffractograms of HZSM-5 and CZA35 are shown in Fig. 1. Fig. 1 indicates the presence of characteristic peaks of crystalline ZSM-5 at $2\theta = 8.0^\circ$, 8.95°, 23.2°, 23.95°, and 25.45°, respectively [16]. The composite CZA35 showed similar XRD pattern as of ZSM-5 indicating that ZSM-5 crystalline structure was retained even after the addition of alumina. There was no significant shift in the characteristic peaks of ZSM-5 suggesting that no strong specific chemical interactions occurred between HZSM-5 and alumina [16]. A decrease in the intensity was observed due to the less amount of HZSM-5 in the composite.

Fig. 2 shows the XRD diffractograms of Al-MCM-41 and its composite with alumina, CMA25 in the 2θ low angle region. The typical

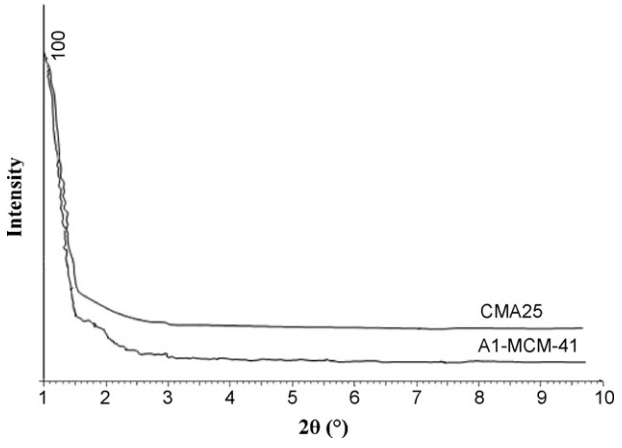

Fig. 2. XRD patterns of Al-MCM-41 and composite CMA25 in the 2θ low angle region.

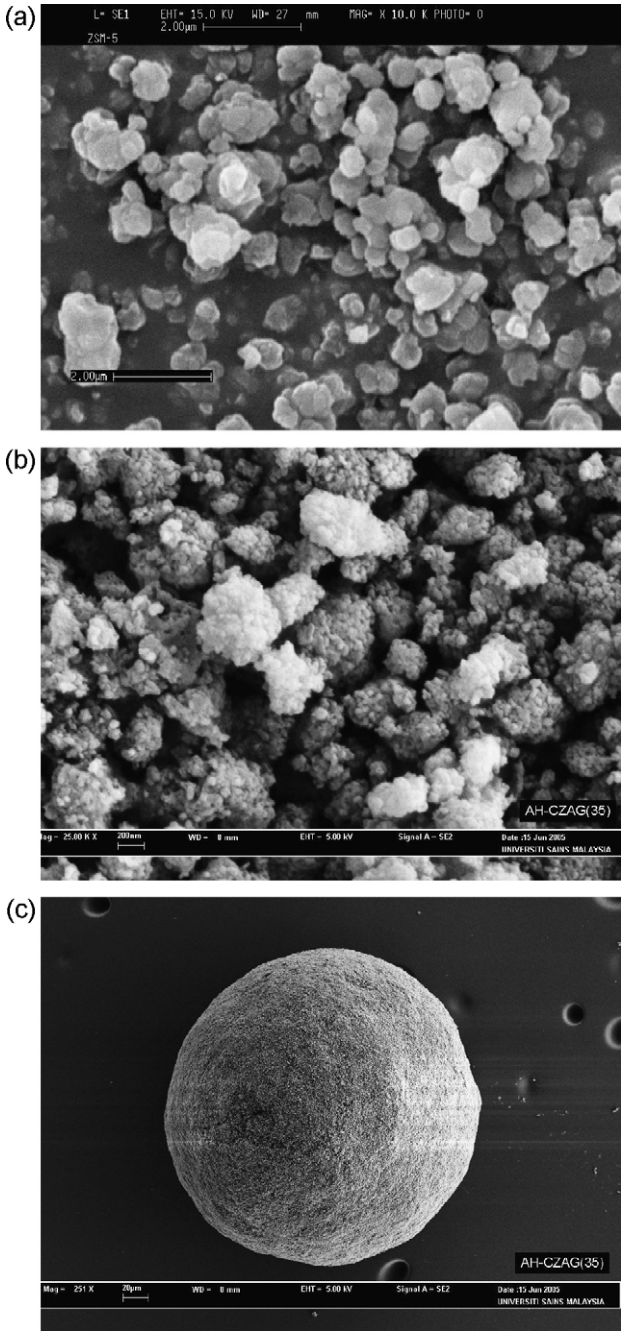

Fig. 3. SEM images of (a) uncoated HZSM-5, (b) surface of composite CZA35 granule and (c) full granular composite CZA35.

XRD pattern of a hexagonal structure of mesoporous material is generally identified with an intense peak and 3-weak peaks at 2θ low angle region ($2\theta < 10^\circ$) [17]. It can be seen from the XRD spectra, Al-MCM-41 retained hexagonal structure due to the presence of main peak (1 0 0) although the structure was not highly ordered due to the absence of other typical peaks. Whereas, the XRD pattern of composite CMA25 was nearly similar as Al-MCM-41 showing that the addition of alumina did not affect Al-MCM-41 structure.

The SEM images in Fig. 3a and b show changes in the morphology of HZSM-5 after granulation with alumina. HZSM-5 exhibited agglomerate particles with flat surfaces (Fig. 3a). With the addition of alumina, the granular composite CZA35 displayed particles with rough surfaces (Fig. 3b). These rough particles are alumina which formed irregular blocks, consisted of small particles of about 1 μm

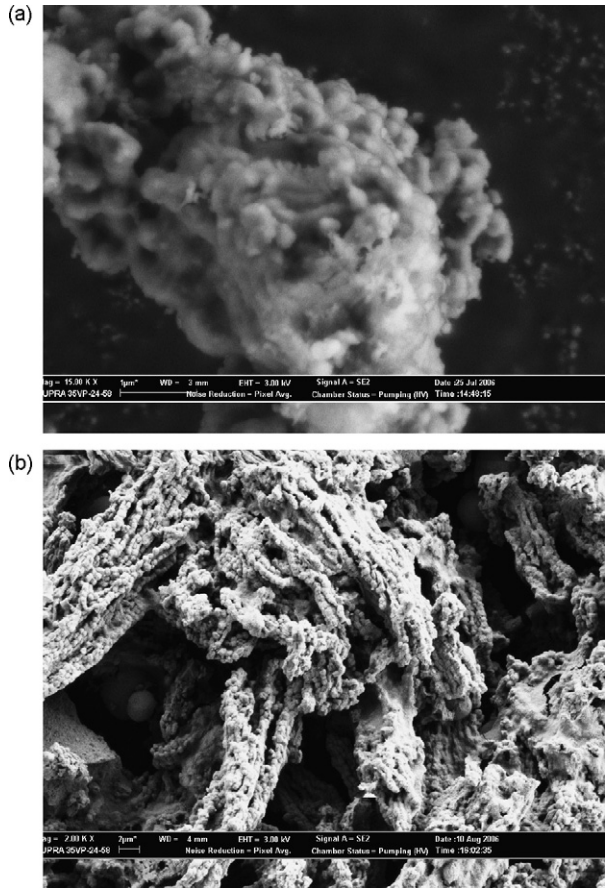

Fig. 4. SEM image of (a) Al-MCM-41 at magnification of 15 K and (b) surface of composite CMA25 at magnification of 2 K.

diameter [18]. These images confirmed that composite granules contained layer of alumina. The surface morphology of full CZA35 granule can be seen from Fig. 3c. Fig. 4 shows SEM micrographs of Al-MCM-41 (Fig. 4a) and CMA25, respectively (Fig. 4b). The rod-like shape morphology of Al-MCM-41 did not appear in CMA25, suggesting that Al-MCM-41 was covered by the other materials.

In order to identify the nature, strength and relative amount of the active sites (Lewis and Brønsted acid sites) present in composite samples, FTIR spectra of the pyridine adsorbed region were obtained and the results are shown in Fig. 5. The ordered aluminosilicate materials after pyridine adsorption exhibited typical

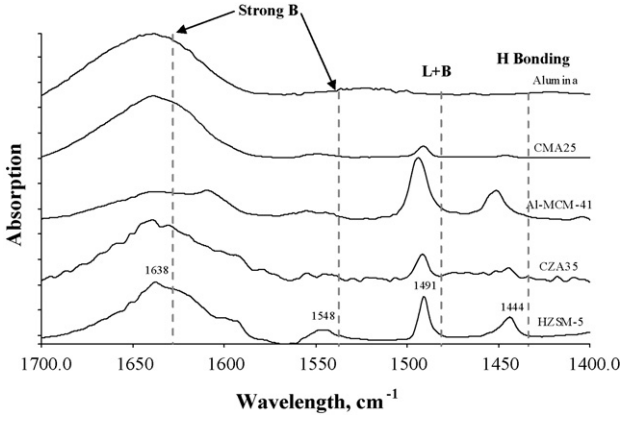

Fig. 5. FTIR for the pyridine-adsorbed HZSM-5, Al-MCM-41, their composites containing alumina: CZA35 and CMA25, and alumina.

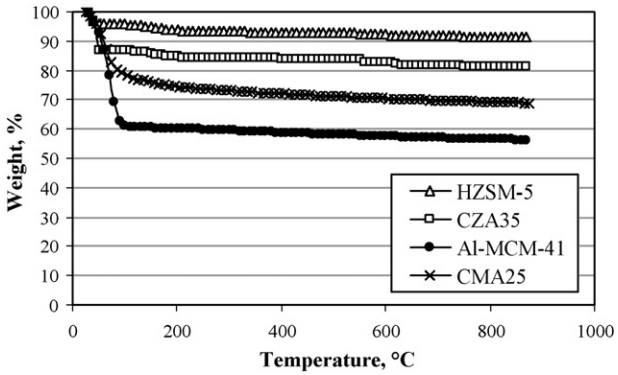

Fig. 6. Thermal gravimetric analysis of HZSM-5, CZA35, Al-MCM-41 and CMA25.

bands due to hydrogen bonded pyridine (1440 cm^{-1}), pyridinium ion ring vibration due to pyridine bound to Brønsted acid sites (1546 and 1637 cm^{-1}) and pyridine associated with the combination of Lewis and Brønsted acidity (1490 cm^{-1}) [19]. All those peaks were observed for HZSM-5 with relatively high intensities. The intense peak was due to the presence of large number of accessible acid sites and thus could adsorb higher amount of pyridine. In case of CZA35 sample, the bands at 1440, 1490 and 1637 cm^{-1} were found with relatively lower intensity than that of HZSM-5. Similar observation in the drop of acidity with increase of alumina was noticed using TPD of ammonia studies [2]. It is noticed that the conversion and gaseous products decreased slightly with the increase in alumina content in both composite catalysts. This was due to lower acidity that suppressed the cracking reaction resulting in lower conversion. However a relatively higher yield of OLP and gasoline fraction was obtained with both composite catalysts.

Fig. 6 shows the thermal gravimetric analysis (TGA) of the catalysts. This analysis was carried out to find out the loss of catalyst weight with the increase of temperature from the room temperature to 1173 K in order to evaluate their thermal stability. A substantial weight reduction was observed for all catalysts at initial analysis due to the moisture removal at 373 K. After moisture removal, the weight percentage of HZSM-5 left was ~93 wt% and CZA35 was ~85 wt% from their initial weight. This observation shows that composite CZA35 retained higher moisture than HZSM-5. However, after 373 K, both catalysts showed stable weight percentage with the increase of temperature (10 K/min) until the maximum temperature, 1173 K. These results show that both catalysts had good thermal stability. In case of composite CMA25, Al-MCM-41 released higher moisture of about 40% from its initial weight as compared to the composite CMA25 which released about 20%. These observations show that Al-MCM-41 adsorbed more water as compared to the composite CMA25. After 373 K, both catalysts gave stable weight with the increase of temperature (10 K/min) until the maximum temperature, 1173 K. This revealed that both catalysts had good thermal stability. However, Al-MCM-41 experienced lower weight loss of about 4% as compared to composite CMA25 which lost 11% weight after the moisture removal once the analysis was completed.

3.2. Catalytic cracking activity studies

The cracking products were mainly organic liquid product (OLP), gaseous product, water and coke. The conversion of palm oil and yield of product are defined as:

$$\text{conversion (wt\%)} = \frac{[\text{gas(g)} + \text{OLP(g)} + \text{water(g)} + \text{coke(g)}]}{\text{palm oil feed(g)}} \times 100 \quad (1)$$

Table 1
Catalytic cracking of palm oil over HZSM-5, CZA35, CMA 25, Al-MCM-41, steamed HZSM-5 (St-ZSM5), steamed composite catalyst CZA35 (St-CZA35), steamed composite catalyst CMA25 (St-CMZA25), steamed Al-MCM-41.

Catalyst	HZSM-5	CZA35	CMA25	Al-MCM-41	St-ZSM5	St-CZA35	St-CMA25	St-Al-MCM-41
Conversion	99	97	79	83	94	92	62	61
Product distribution (wt%)								
Gas	26	20	11	15	16	13	6	7
OLP	65	71	57	55	69	72	47	37
Water	7	5	6	6	6	5	4	4
Coke	1	1	5	7	3	2	5	13
Yield of OLP (wt%)								
Gasoline fraction	45	47	37	34	46	46	20	13
Kerosene fraction	17	20	15	15	20	22	17	18
Diesel fraction	3	4	5	6	3	3	10	6

$$\text{yield (wt\%)} = \frac{\text{desired product(g)}}{\text{palm oil feed(g)}} \times 100 \quad (2)$$

Table 1 presents the conversion, yield of gasoline and yield of coke over different catalysts tested. The steam treated composite CZA35 (St-CZA35) showed its relatively stable activity with 92 wt% palm oil conversion. This value was 5 wt% lower than that obtained over fresh composite CZA35. The gasoline fraction was slightly dropped by 1 wt% in comparison with the fresh composite. Same observation was also found for steam treated ZSM-5 (St-ZSM5) with 94 wt% palm oil conversion which dropped by 5 wt% as compared with the fresh HZSM-5 while gasoline fraction yield was 46.0 wt%, slightly increased as compared to the fresh catalyst. These results show that composite CZA35 structure did not change after steam treatment and activity remained nearly same as fresh composite catalyst.

Composite CMA25 and steam treated composite CMA25 (St-CMA25) showed higher stability compared to steam treated Al-MCM-41 (St-AlMCM-41) based on its higher cracking activity. St-CMA25 gave 62 wt% palm oil conversion with 20 wt% gasoline fraction yield and 5 wt% coke; while the oil conversion over St-AlMCM-41 was 61 wt%, gasoline fraction yield of 13 wt% and 13 wt% coke. The conversion after steam treatment suggests the changes in the MCM-41 mesostructure. The improved hydrothermal stability was due to the presence of alumina (less ordered mesoporous materials) in the composite granule protecting the Al-MCM-41 (core) and this could be observed in the SEM analysis. The lower hydrothermal stability of Al-MCM-41 could be due to its mesostructure affected by high uptake of moisture, even though its thermal stability was comparable with the composite.

3.3. Deactivation studies

The conversion of palm oil over fresh HZSM-5, Al-MCM-41 and their composites with alumina (CZA35 and CMA25) are presented in Fig. 7. The catalytic activity of all catalysts dropped with time on stream due to the coke formation and its deposition on the catalyst. The stability of the catalysts structure also had significant effect on their activity since the catalysts were exposed to high temperature for long reaction time. The catalysts showed different deactivation behaviors (Fig. 7). Some catalyst followed the linear deactivation law whereas some catalysts followed exponential and hyperbolic deactivation laws. It is reported in the literature that the cracking of gas oil followed the exponential law and also depends over time on stream operation [20,21]. However this assumption was not true for the present palm oil cracking study. The cracking mechanism in palm oil differs from gas oil cracking because of the presence of different types of fatty acid glycerides. The gas oil is relatively heavier than palm oil and also contains sulfur and heavy metals such as vanadium [20].

Fig. 8 shows that CZA35 and CMA25 deactivated with lower deactivation rate as compared to their microporous (HZSM-5) or mesoporous (MCM-41) catalysts respectively. Although CZA35 and CMA25 had lower acidity, but the presence of alumina enhanced thermal and hydrothermal stability of the catalysts resulting in lower deactivation rates. The higher deactivation rate of Al-MCM-41 was due to its mesostructure. The presence of low order alumina may explain this result since Al-MCM-41 without alumina addition deactivated at faster rate than its composite, CMA25. The mild acidity of CMA25 still allows the cracking to occur and hence the small pre-cracked molecules could access Al-MCM-41 through the macropores of alumina present in CMA25. The addition of alumina and its presence acted as a protection layer towards the mesostructure of Al-MCM-41. The presence of alumina in HZSM-5 and Al-MCM-41 lowered initial cracking rate due to the drop in the acid sites of composite catalysts and thus lowered the deactivation of catalysts.

In order to determine the deactivation rate of the catalysts, a deactivation model is proposed by assuming that the catalyst activity (φ) defined as the ratio of the rate of reaction at time t to the rate of reaction over fresh catalyst ($t = 0$). The activity is dependent on the time on stream (TOS), t. The rate of deactivation is presented as [22]:

$$\frac{d\varphi}{dt} = -k_d \varphi^{n_d} \quad (3)$$

where φ = catalyst activity is defined as follows:

$$\varphi(t) = \frac{\text{rate of reaction at time } (t = t)}{\text{rate of reaction at time } (t = 0)} \quad (4)$$

where φ = catalyst activity, k_d = deactivation rate constant (h^{-1}) and n_d = order of catalyst deactivation. The values of n_d (for case of $n_d > 2$) and k_d were estimated using non-linear regression analysis method based on Levenberg–Marquard's algorithm for all activity models

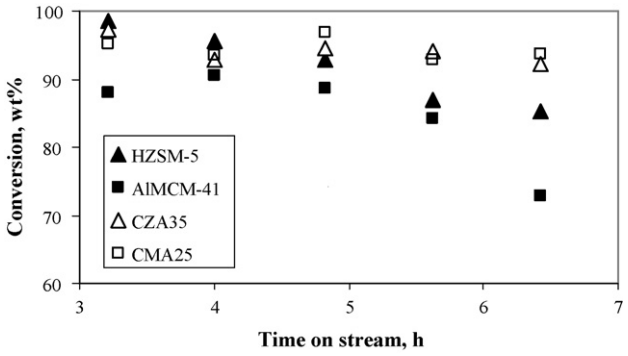

Fig. 7. Time on stream data for the cracking of palm oil over different types of catalysts.

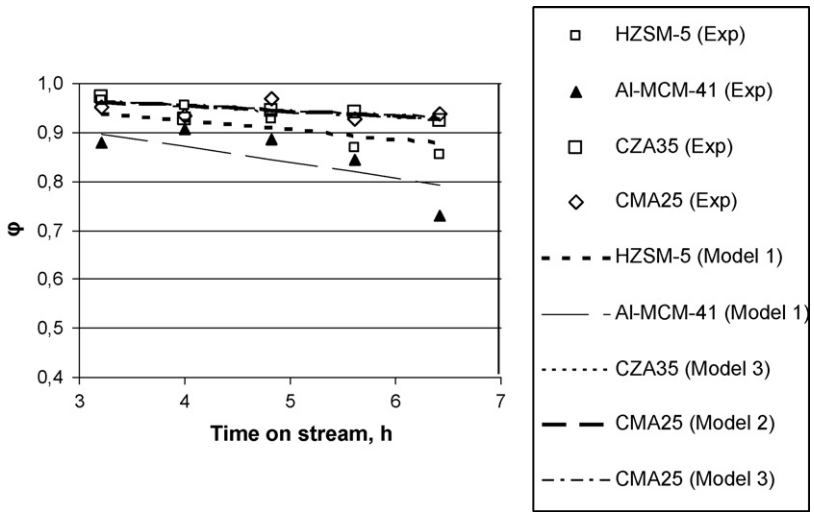

Fig. 8. Experimental and prediction data of palm oil cracking activity over different types of catalysts.

[20]. Four types of activity models (φ): linear ($n_d = 0$), exponential ($n_d = 1$), hyperbolic ($n_d = 2$) and polynomial ($n_d > 2$) were applied in order to find out the best model representing the experimental data of catalyst deactivation. Table 2 presents the values of deactivation rate constant, k_d, reaction order, n_d calculated from the best fitted model. The value of k_d and n_d varied with type of cracking catalyst used. It is can be seen that the deactivation order, n_d of both composites was higher than that of their microporous or mesoporous catalysts. The deactivation order of HZSM-5 and Al-MCM-41 was 0, showing these catalysts deactivated linearly with time on stream (TOS). However, in case of composites, they fitted two models well, those are exponential ($n_d = 1$) and hyperbolic ($n_d = 2$). It can be observed that both composite CZA35 and CMA25 deactivated with lower deactivation rate constant of 0.0125 and 0.0116 h^{-1} respectively. The higher deactivation rate constant of Al-MCM-41 was due to its mesostructure which was responsible for higher coke formation. Fig. 8 shows the comparative plot of predicted activity obtained using the estimated values of n_d and k_d with the experimental data. The experimental activity data of all catalysts distributed close to the chosen model line data except for Al-MCM-41 due to its higher sum of error squares (Σs^2) as compared to others catalysts.

The yield of desired product, gasoline fraction, was the main concern in determining the most efficient catalyst. Fig. 9 shows the reaction time dependency for the yield of gasoline fraction over Al-MCM-41 and CMA25 catalysts. There was a correlation between the yield of gasoline fraction over Al-MCM-41 with the conversion. Conversely, in case of CMA25, there was no correlation between the gasoline fraction yield and palm oil conversion. The gasoline yield over Al-MCM-41 and CMA25 decreased with TOS. This trend is common in cracking process due to the catalyst deactivation and dropping in cracking activity towards the lighter products. Overall, CMA25 produced lower yield of gasoline fraction as compared to Al-MCM-41. This revealed that the acidity also played an important role in gasoline production. This was reported in the cracking of paraffin where the product chain length was dependent on the strength of the Brønsted sites [23]. On the other hand, the range of gasoline yield produced over these two catalysts was quite similar as can be observed from the maximum and minimum value of gasoline yield. CMA25 gave gasoline fraction yield of 37 wt% at the beginning of the reaction time and dropped to the lowest gasoline yield of 21 wt% after 5.6 h of TOS, while Al-MCM-41 gave a maximum yield of gasoline as 38.7 wt% at 4 h TOS but dropped to the lowest gasoline yield of 21.7 wt% after 6.4 h of TOS. However, due to the significant drop in gasoline yield over CMA25 at 4, 4.8 and 5.6 h of TOS in comparison with Al-MCM-41, CMA25 was not selective towards gasoline fraction.

Fig. 10 shows the reaction time dependency for the yield of gasoline fraction over HZSM-5 and composite CZA35. The gasoline yield dropped with time on stream (TOS). It can be observed that CZA35 gave comparable and higher gasoline yield at certain TOS as compared with HZSM-5. Due to this result, the yield of gasoline fraction over these two regenerated catalysts was also studied. CZA35 gave gasoline fraction yield as 47 wt% at the beginning of the reaction time. The gasoline yield dropped to 36 wt% after 5.62 h of TOS, since the catalyst was deactivated and more coke was deposited at the active sites. HZSM-5 gave a maximum gasoline yield of 44 wt% at 4.02 h of TOS and slightly dropped to the lowest gasoline yield of 41 wt% after 6.42 h of TOS in cycle I. Although the palm oil conver-

Table 2
Deactivation rate constant, k_d and deactivation order, n_d for different catalysts calculated from the best fitted model.

Catalyst	Model	n_d	k_d
HZSM-5	$\varphi = 1 - k_d t$	0	0.0190
CZA35	$\varphi = \exp(-k_d t)$	1	0.0125
CZA35	$\varphi = 1/(1 + k_d t)$	2	0.0128
Al-MCM-41	$\varphi = 1 - k_d$	0	0.0322
CMA25	$\varphi = \exp(-k_d t)$	1	0.0116
CMA25	$\varphi = 1/(1 + k_d t)$	2	0.0118

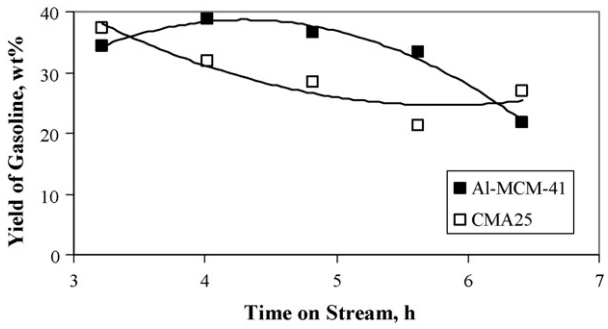

Fig. 9. Time on stream gasoline yield from the cracking of palm oil over Al-MCM-41 and composite CMA25.

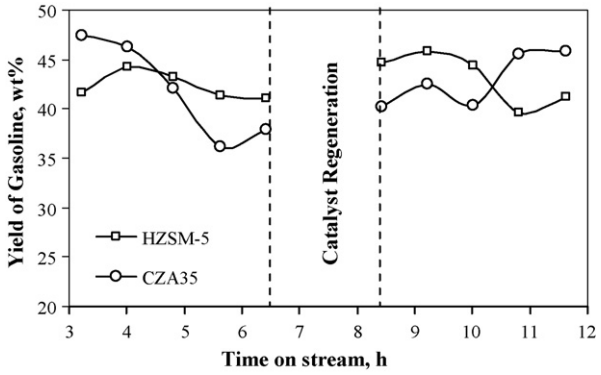

Fig. 10. Time on stream gasoline yield from the cracking of palm oil over the fresh and regenerated HZSM-5 and composite CZA35.

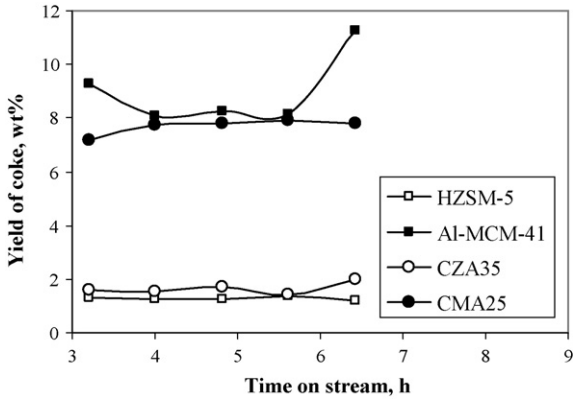

Fig. 11. Time on stream coke yield over the catalysts from the cracking of palm oil.

sion over CZA35 dropped after regeneration and experienced higher gasoline fraction yield drop than HZSM-5 in cycle I, however, CZA35 gave the highest gasoline fraction yield at the end of the reaction time after regeneration (cycle II) (46 wt%). After regeneration, the gasoline fraction yield decreased except for CZA35 gasoline fraction yield due to the changes in the catalyst structure. The regenerated HZSM-5 gave only high gasoline fraction yield at the beginning of cycle II but dropped after subjected to the longer reaction time.

The catalyst improvement in terms of resistance to coking, the composite CMA25 was less susceptible to coke as compared to Al-MCM-41 due to lower coke production in CMA25 as depicted in Fig. 11. Fig. 11 shows the amount of coke (wt%) produced over different catalysts with TOS. The lower coke production by CMA25 is one of the reasons for its higher and stable conversion with TOS than Al-MCM-41. The open structure of MCM-41 eased the deposition of coke precursor and resulted in high coke content. The presence of alumina reduced the coke production due to the changes in the porous structure of CMA25. For composite CZA35, even it produced higher coke fraction than HZSM-5, however the amount was not appreciable. This explains that the performance of CZA35 was comparable with HZSM-5.

The composite CZA35 (65 wt% HZSM-5) showed comparable cracking activity in terms of hydrothermal stability, deactivation and selectivity towards gasoline fraction as compared with HZSM-5. The composite CMA25 (75 wt% Al-MCM-41) also gave higher activity, hydrothermal stability and stable activity with TOS as compared with 100 wt% Al-MCM-41 even it was not selective towards gasoline production.

4. Conclusions

CZA35 and CMA25 composites deactivated with lower deactivation rate as compared to their microporous (HZSM-5) or mesoporous catalysts (MCM-41) respectively. The presence of low order alumina enhanced hydrothermal stability and lowered the acidity of composites. The changes in the porous structure of composite CMA25 made it less susceptible to coke formation, thus resulting in the lower deactivation rates. CZA35 gave comparable activity, hydrothermal stability and selectivity towards gasoline formation as parent HZSM-5 catalyst, thus addition of alumina in HZSM-5 is beneficial in terms of better stability and deactivation without affecting the yield of gasoline fraction.

Acknowledgements

The authors would like to acknowledge the research grant provided by the Ministry of Science, Technology and Environment, Malaysia under long term IRPA grant (project: 02-02-05-2184 EA005) and eScience fund that has resulted in this article. The authors would also like to acknowledge Universiti Sains Malaysia for providing research grant under Research University (RU) grant scheme.

References

[1] F.A. Twaiq, N.A.M. Zabidi, S. Bhatia, Catalytic conversion of palm oil to hydrocarbons: performance of various zeolite catalysts, Ind. Eng. Chem. Res. 38 (1999) 3230–3237.
[2] F.A. Twaiq, A.R. Mohamed, S. Bhatia, Liquid hydrocarbon fuels from palm oil by catalytic cracking over aluminosilicate mesoporous catalysts with various Si/Al ratios, Micropor. Mesopor. Mater. 64 (2003) 95–107.
[3] F.A. Twaiq, N.A.M. Zabidi, A.R. Mohamed, S. Bhatia, Catalytic conversion of palm oil over mesoporous aluminosilicate MCM-41 for the production of liquid hydrocarbon fuels, Fuel Process Technol. 84 (2003) 105–120.
[4] F.A. Twaiq, A.R. Mohamed, S. Bhatia, Performance of composite catalysts in palm oil cracking for the production of liquid fuels and chemicals, Fuel Process Technol. 85 (2004) 1283–1300.
[5] Y.S. Ooi, F.A. Twaiq, R. Zakaria, A.R. Mohamed, S. Bhatia, Biofuel production from catalytic cracking of palm oil, Energy Sources 25 (2003) 859–869.
[6] Y.S. Ooi, R. Zakaria, A.R. Mohamed, S. Bhatia, Catalytic conversion of palm oil based fatty acid mixture to liquid fuel, Biomass and Bioenergy 27 (2004) 477–484.
[7] Y.S. Ooi, R. Zakaria, A.R. Mohamed, S. Bhatia, Hydrothermal stability and catalytic activity of mesoporous aluminum-containing SBA-15, Catal. Commun. 5 (2004) 441–445.
[8] Y.S. Ooi, R. Zakaria, A.R. Mohamed, S. Bhatia, Synthesis of composite material MCM-41/Beta and its catalytic performance in waste used palm oil cracking, Appl. Catal. A: Gen. 274 (2004) 15–23.
[9] J.S. Buchanan, D.H. Olson, S.E. Schramm, Gasoline selective ZSM-5 FCC additives: effects of crystal size, SiO_2/Al_2O_3, steaming, and other treatments on ZSM-5 diffusivity and selectivity in cracking of hexene/octene feed, Appl. Catal. A: Gen. 220 (2001) 223–234.
[10] J.W. Gosselink, J.A.R. van Veen, in: B. Delmon, G.F. Froment (Eds.), Catalyst Deactivation, Elsevier, Amsterdam, 1999, pp. 3–16.
[11] H. Liu, H. Zao, X. Gao, J. Ma, A novel FCC catalyst synthesized via in situ overgrowth of NaY zeolite on kaolin microspheres for maximizing propylene yield, Catal. Today 125 (2007) 163–168.
[12] Y.S. Lin, G. Buelna, Sol–gel-derived mesoporous γ-alumina granules, Micropor. Mesopor. Mater. 30 (1999) 359–369.
[13] B. Lindlar, A. Kogelbauer, R. Prins, Chemical, structural, and catalytic characteristics of Al-MCM-41 prepared by pH-controlled synthesis, Micropor. Mesopor. Mater. 38 (2000) 167–176.
[14] Y.S. Lin, Z. Yang, Sol–gel synthesis of silicalite/γ-alumina granules, Ind. Eng. Chem. Res. 39 (2000) 4944–4948.
[15] L.M. Huang, Q.Z. Li, Improvement on thermal stability and acidity of mesoporous materials with post-treatment of phosphoric acid, Stud. Surf. Sci. Catal. 129 (2000) 93–98.
[16] P. Borges, R. Pinto, M.A.N.D.A. Lemosa, F. Lemos, J.C. Vedrinec, E.G. Derouaned, F.R. Ribeiro, Activity–acidity relationship for alkane cracking over zeolites: *n*-hexane cracking over HZSM-5, J. Molec. Catal. A: Chem. 229 (2005) 127–135.
[17] R. Ryoo, J.M. Kim, Structural order in MCM-41 controlled by shifting silicate polymerization equilibrium, J. Chem. Soc. Chem. Commun. 8 (1995) 711–712.
[18] K. Gora-Marek, M. Derewinski, P. Sarv, J. Datka, IR and NMR studies of mesoporous alumina and related aluminosilicates, Catal. Today 101 (2005) 131–138.

[19] B. Chakraborty, B. Viswanathan, Surface acidity of MCM-41 by in situ IR studies of pyridine adsorption, Catal. Today 49 (1999) 253–260.
[20] J. Ancheyta-Juarez, F. Lopez-Isunza, E. Aguilar-Rodriguez, J.C. Moreno-Mayorga, A strategy for kinetic parameter estimation in the fluid catalytic cracking process, Ind. Eng. Chem. Res. 36 (1997) 5170–5174.
[21] M.A. Abul-Hamayel, Kinetic modeling of high-severity fluidized catalytic cracking, Fuel 82 (2003) 1113–1118.
[22] H.S. Fogler, Elements of Chemical Reaction Engineering, 3rd edition, Prentice Hall International, 1999.
[23] K.A. Gumming, B.W. Wojciechowski, Hydrogen transfer, coke formation, and catalyst decay and their role in the chain mechanism of catalytic cracking, Catal. Rev. Sci. Eng. 38 (1996) 101–157.